

Deciphering the role of Fe impurities in the electrolyte boosting the OER activity of LaNiO₃

Haritha Cheraparambil¹, Miquel Vega-Paredes², Yue Wang¹, Harun Tüysüz¹, Christina Scheu²,
Claudia Weidenthaler ^{1*}

¹ Max-Planck-Institut für Kohlenforschung, Kaiser-Wilhelm-Platz 1, D-45470 Mülheim an der Ruhr, Germany

² Max-Planck-Institut für Eisenforschung, Max-Planck-Straße 1, D-40237 Düsseldorf, Germany

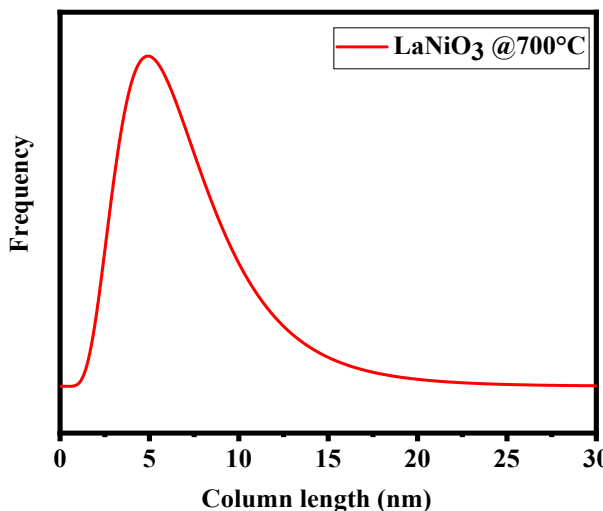


Figure S1. Column length distribution of LaNiO₃ obtained at 700 °C.

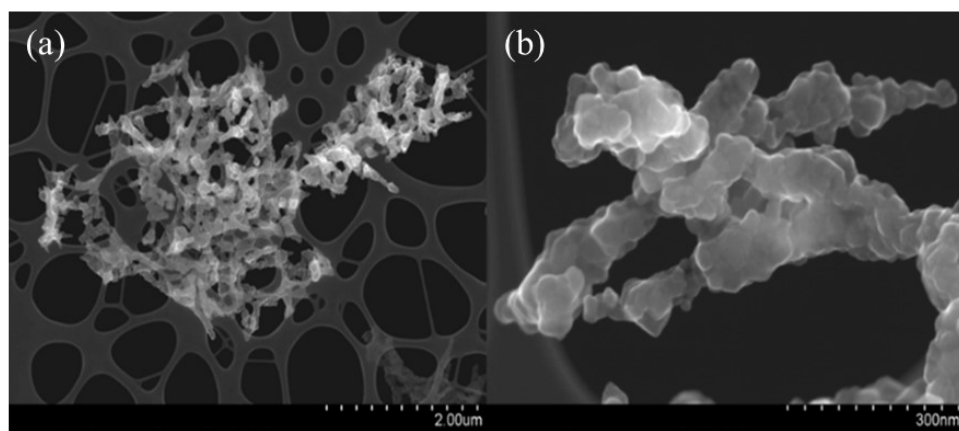


Figure S2. Scanning electron microscopy images of LaNiO₃ shown in different magnifications (a) and (b).

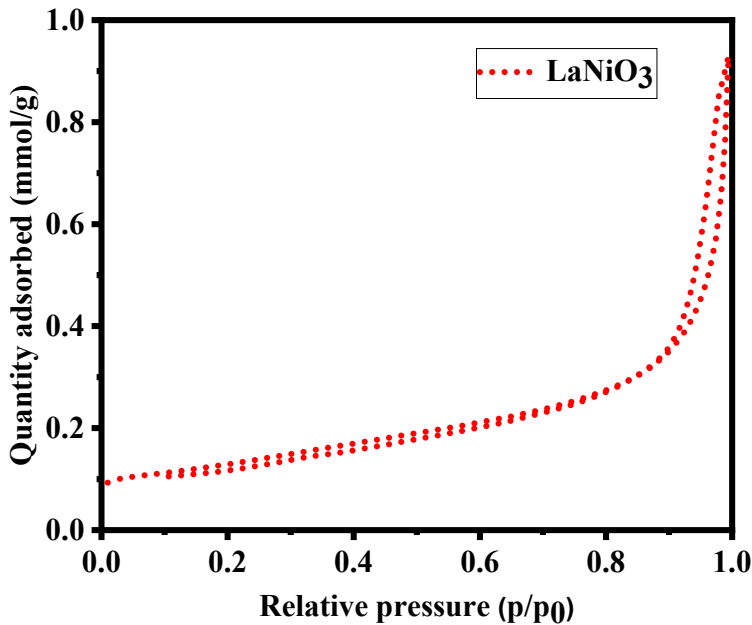


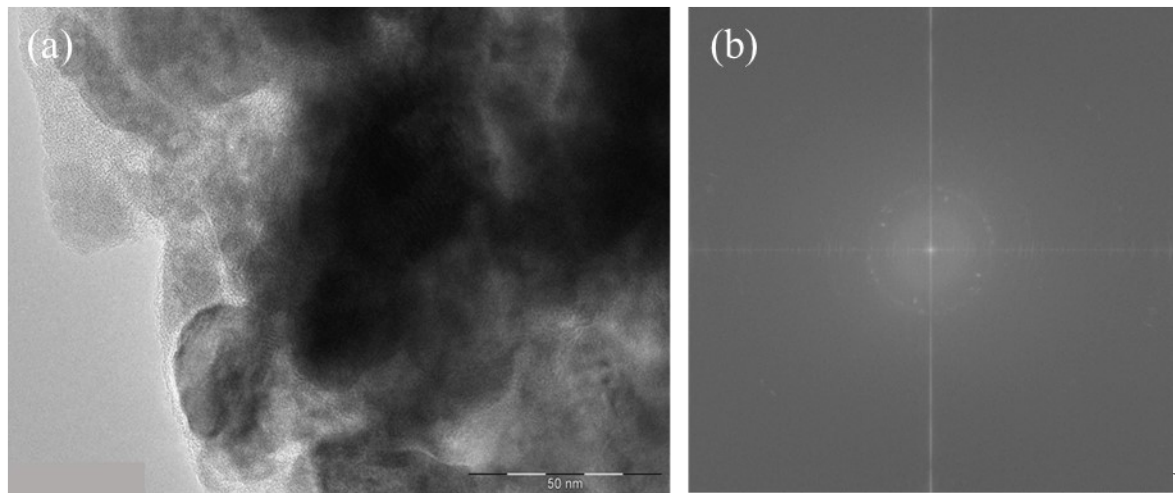
Figure S3. Nitrogen physisorption isotherms of LaNiO₃.

Electrolyte	Fe /ppm
1 M commercial KOH solution	0.43
Purified KOH solution	0.005
Purified KOH solution + 1 ppm Fe	1.34
Purified KOH solution + 3 ppm Fe	3.22
Purified KOH solution + 7.5 ppm Fe	7.60
Purified KOH solution + 10 ppm Fe	10.65

Table S1. ICP-OES data of 1 M KOH under controlled addition of Fe impurities.

Samples	R_{electrolyte} /Ω	R_{ct} /Ω
Purified KOH solution	1.5	10.8
Purified KOH solution + 1 ppm Fe	1.5	4.5
Purified KOH solution + 3 ppm Fe	1.4	1.4
Purified KOH solution + 7.5 ppm Fe	1.4	0.6
Purified KOH solution + 10 ppm Fe	1.8	1.1

Table S2. Nyquist plot fits using the Randles circuit.



e S4. (a) TEM image and (b) its corresponding Fast Fourier Transform (FFT) of LaNiO_3 obtained after the stability test. The presence of reflections in the FFT indicates that the crystallinity is preserved during the stability test.

Raman shift /cm ⁻¹	Vibrational modes
~156	Internal vibration of La
~209	Rotational vibration corresponding to structural distortion
~400, ~451	Vibration modes of the oxygen octahedra
~474, ~555	Bending and stretching modes of Ni-O in NiOOH ¹
~825	O-O stretch of adsorbed *O-OH species on the Au surface ²

Table S3. Different Raman modes of LaNiO₃.^{3,4}

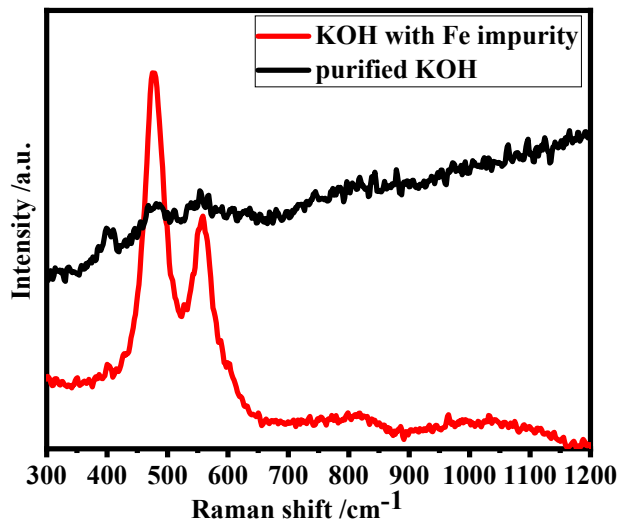


Figure S5. Comparison of Raman spectra of LaNiO₃ with the one obtained at a potential of 1.5 V in 1 M KOH with additional Fe impurities.

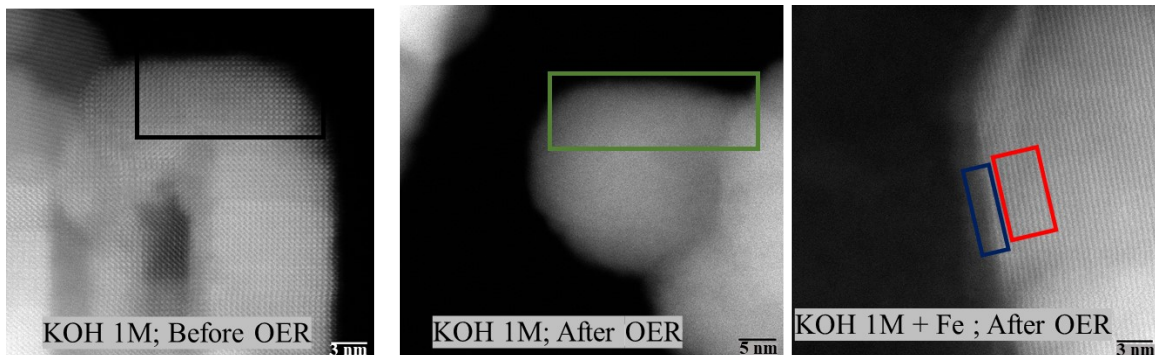


Figure S6. STEM images of LaNiO_3 under different conditions. The EELS spectra are collected from the respective marked regions; before OER (black colour), after OER in 1M KOH (green colour), nanoparticles after OER in 1M KOH with Fe impurities, the amorphous layer formed after OER in 1M KOH with Fe impurities.

Sample	La (ppm)	Ni (ppm)	Fe (ppm)
Electrolyte before OER	-	-	7.6
Electrolyte after OER	0.4	-	5.8

Table S4. ICP-OES data of the electrolyte before and after OER.

REFERENCES

1. L. Trotochaud, S. L. Young, J. K. Ranney and S. W. Boettcher, *J Am Chem Soc*, 2014, **136**, 6744-6753.
2. E. Budiyanto, S. Salamon, Y. Wang, H. Wende and H. Tuysuz, *JACS Au*, 2022, **2**, 697-710.
3. N. Chaban, M. Weber, S. Pignard and J. Kreisel, *Applied Physics Letters*, 2010, **97**.
4. A. Schober, J. Fowlie, M. Guennou, M. C. Weber, H. Zhao, J. Íñiguez, M. Gibert, J.-M. Triscone and J. Kreisel, *APL Materials*, 2020, **8**.